Bond Graph Modeling, Simulation and Analysis of the Rotating Duct

P.K.Kaushik, S.C. Sati, Rajeev Jain
ADRDE (DRDO)
Agra-282001, India
pkkiitkgp@gmail.com, scsati@rediffmail.com,
rajeevjain5555@rediffmail.com

A.Mukherjee
Indian Institute of Technology Kharagpur
Kharagpur-721302, India
amalendu.htc@gmail.com

***Abstract*- This paper present bond graph modeling of the rotating duct. In this paper emphasis is given on the modeling of duct that is rotating about its axis and simultaneously discharging water. Basically this is the fluid dynamics problem, so first it is approximated as a hydraulics problem. The duct may be of any shape. The fluid flows through the duct by centrifugal body forces. The analysis of this complex situation is made tractable by use of bond graph modeling. The bond graph is created by taking pressure and torque as an effort variable in hydraulic and mechanical domain respectively. Discharge or volume flow rate and angular velocity as flow variable in hydraulic and mechanical domain respectively. Simulations are performed on software SYMBOLS Sonata [7] to study the effects of different geometric and operating parameters on the performance of the driving motor. In this paper simplified situation of the duct is considered and dynamics of the rotating mechanism is neglected. The practical application of the rotating duct is to find the power required to drive the radial flow pump assuming one duct as one sector of the impeller of the pump.**

Keywords- Bond graph; Viscous resistance; Bernoulli resistance; Fluid dynamics.

I. INTRODUCTION

Main object of this paper is to find the power consumption by motor for rotating the duct and study the effects of design parameters on the performance of the motor.

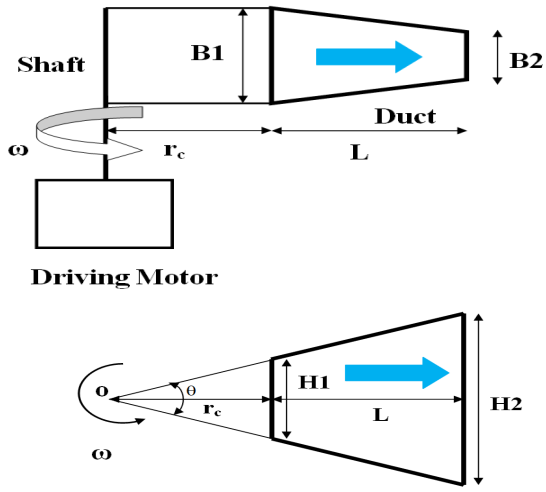

Fig.1: Rotating duct.

The duct is rotating by driving motor simultaneously discharging water. as shown in Fig 1.
The water from the duct will flow radially due to centrifugal body forces. The analysis of this complex situation is made tractable by use of bond graph modeling.

Detailed analysis shows that apart from total effective fluid inertia there are two kinds of resistances governing the flow, one viscous resistance and other may be called Bernoulli resistance. [1, 2].

Thus on the fluid one part of inertia force is due to local rate of change of discharge depicted as an inertial element and convective part of inertial force gives rise to Bernoulli resistance. The so called Bernoulli resistance for divergent passages may even be negative and for fast flow may become larger in magnitude than effective viscous forces leading to overall effective negative net resistance. In such a situation pattern of flow will become unstable and would settle in another stable flow pattern [1, 2, 3]. In the case of fast rotating duct, this pattern may become a parallel sets of jets confined to one side of the passages leading to zero Bernoulli resistance in each such passage. This issue is discussed in this paper. The total resistive torque on the shaft of the driving motor is due to transfer of fluid momentums at the exit from the duct and at the entry. The other components of resistive torque on the shaft would be due to Coriolis acceleration and radial flow of fluid inside a rotating passage [5]. In this paper simplified situation of the duct is considered and dynamics of rotating mechanism is neglected. A bond graph model is created which includes all these aspects.

Table 1:Nomenclature.

B_1 = B1=Wbld1	Width of duct at inner end (m)
B_2 =B2=Wbld2	Width of duct at outer end (m)
H_1 =H1	Gap between two sides of duct at inner end (m)
H_2 =H2	Gap between two sides of ducts at outer end (m)
r_c	Inner radius of duct (m)
L=Lbld	Length of duct (m)
ρ	Density of fluid (kg/m^3)
μ	Dynamic viscosity of fluid (Pa-s)
N	Angular speed of the driving motor (RPM)
$\dot{Q}$	Volume flow rate (m^3/s)

RadFl_Fact= RadFlfact	Radial flow factor
TanFl_Fact= TanFlfact	Tangential flow factor
Radd_Fact	Additional resistance factor

II . ASSUMPTIONS

Following assumptions are made in the model.
1. Effects of rotating arrangements are neglected.
2. Fluid flow direction is assumed to be in the direction of stream line.
3. Properties of the fluid assumed to be constant.

III. THEORY AND BOND GRAPH OF SUB-SYSTEMS

The duct is analyzed using basic fluid flow governing equation for an arbitrary shaped rigid duct. Mukherjee et al. drive the fluid flow governing equation for hydraulic circuit. To model the rotating duct we are using the same concept.

A. Bond graph modeling of hydraulic circuit

Assuming the flow in a rigid tube of arbitrary shape though sufficiently smooth, the flow equation can be written as follow [1].

$$\Rightarrow \left\{\left(\int_0^l \rho \frac{1}{A(\xi)} d\xi\right)\ddot{Q}\right\}\dot{Q} + \left\{\rho\frac{1}{2}\left(\frac{1}{A^2(l)} - \frac{1}{A^2(0)}\right)\dot{Q}^2\right\}\dot{Q} - \left\{\left(\int_0^l \frac{\beta(\xi)}{A(\xi)} d\xi\right)\dot{Q}\right\}\dot{Q} - \left\{\int_0^l B(\xi)\bar{e}_b(\xi).\bar{\eta}(\xi) d\xi\right\}\dot{Q} - P_A\dot{Q} + P_B\dot{Q} = 0 \quad (1)$$

Where,
ξ is distance along the stream line and A (0), A (l) area of the duct at inlet and outlet respectively, $\bar{B}$ is the external body force acting on the fluid per unit volume, $\bar{\eta}$ is unit outer normal at a surface point, $\bar{e}_b$ is unit vector along the direction of body force, P_A and P_B pressure at inlet and outlet of the duct respectively.

Fig. 2 is the bond graph representation of equation (1), [2].

B. Viscous Resistance

Considering the flow through the duct shown in Fig. 3 as fully developed laminar flow between vertical sides of the duct, we can reduce momentum equation as follows.

$$-\frac{\partial P}{\partial x} + \frac{\partial \tau_{xy}}{\partial y} = 0 \quad (2)$$

The shear stress varies linearly with y, Let U is the mean velocity of flow, P is the pressure.

$$\therefore \tau = \mu \frac{\partial U}{\partial y}$$

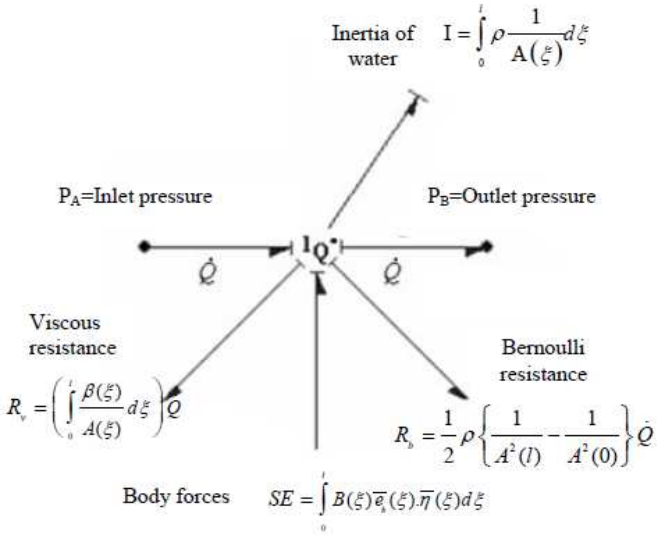

Fig. 2: Bond graph of flow through passage. [1, 2].

Eq. (2) can be written as $\mu \frac{\partial^2 U_x}{\partial y^2} = \frac{\partial P}{\partial x}$ or, $\frac{\partial^2 U_x}{\partial y^2} = \frac{1}{\mu}\frac{\partial P}{\partial x}$

Integrating the above equation $U_x = \frac{1}{2\mu}\frac{\partial P}{\partial x}\left(y^2 - Hy\right)$

Water flow rate $\dot{Q} = \int_0^H U_x B dy \quad (3)$

$$\dot{Q} = -\frac{1}{12\mu}\frac{\partial P}{\partial x} BH^3 \qquad \therefore \frac{\partial P}{\partial x} = -\frac{12\mu\dot{Q}}{B}\frac{1}{H^3}$$

$$H = H_1 + \alpha x, \qquad \alpha = \frac{H_2 - H_1}{L}$$

$$\int_{P_1}^{P_2} \frac{\partial P}{\partial x} dx = -\frac{12\mu\dot{Q}}{B}\int_0^L \frac{dx}{\left(H_1 + \alpha x\right)^3}$$

Let, $H_1 + \alpha x = l'$, $dx = \frac{dl'}{\alpha}$, at $x = 0$, $l' = H_1$

and at $x = l$, $l' = H_2$

$$P_2 - P_1 = -\frac{12\mu\dot{Q}}{B\alpha}\int_{H_1}^{H_2} l'^{-3} dl'$$

$$P_1 - P_2 = \frac{6\mu\dot{Q}}{B\alpha}\left[\frac{1}{H_1^2} - \frac{1}{H_2^2}\right]$$

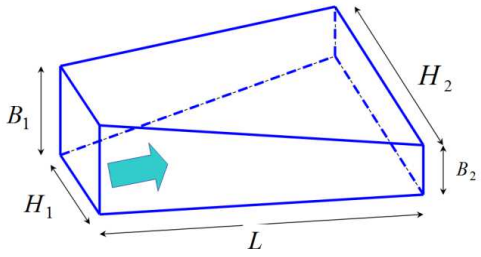

Fig. 3: Assumed shape of the duct.

$$P_1 - P_2 = \left(\frac{6\mu L}{B} \frac{(H_1 + H_2)}{H_1^2 H_2^2} \right) \dot{Q} \tag{4}$$

Hence viscous resistance of side surfaces of the duct

$$R_{v_1} = \frac{6\mu L}{B} \left(\frac{H_1 + H_2}{H_1^2 H_2^2} \right) \tag{5}$$

Let angle between two vertical sides of the duct is θ (6)

Viscous resistance of bottom and top surfaces of the duct

Thus gap between vertical surfaces of the duct at inlet

$$H_1 = 2r_c \sin\frac{\theta}{2} \tag{7}$$

Gap between vertical surfaces of the duct at outlet

$$H_2 = 2\left(r_c + L\right)\sin\frac{\theta}{2} \tag{8}$$

Viscous resistance of top and bottom surfaces of the duct

$$R_{v_2} = \frac{12\mu L}{H_1 + H_2} \left(\frac{B_1 + B_2}{B_1^2 B_2^2} \right) \tag{9}$$

Total viscous resistance using Eq. (5) and Eq. (9)

$$R_v = R_{v_1} + R_{v_2}$$

$$Rv = \frac{12\mu L}{B_1 + B_2} \left(\frac{H_1 + H_2}{H_1^2 H_2^2} \right) + \frac{12\mu L}{H_1 + H_2} \left(\frac{B_1 + B_2}{B_1^2 B_2^2} \right) \tag{10}$$

Additional Resistance

The radial flow of fluid through duct depends on the resistance. This resistance can be varied by adding one additional resistance to viscous and Bernoulli resistance. This additional resistance can be incorporated by wire mesh or perforated plate. This resistance is designated by the factor by which the resistance has increase over the viscous resistance.

Additional resistance= Viscous resistance × Radd_Fact.

C. Bernoulli Resistance

Expression of Bernoulli resistance for the duct referring the Eq. (1).

$$R_b = \frac{1}{2}\rho \left\{ \frac{1}{A^2(l)} - \frac{1}{A^2(0)} \right\} \dot{Q} \tag{11}$$

$$R_b = \frac{1}{2}\rho \left\{ \frac{1}{B_2^2 H_2^2} - \frac{1}{B_1^2 H_1^2} \right\} \dot{Q}$$

$$R_b = \frac{\rho}{2} \left\{ \frac{B_1^2 H_1^2 - B_2^2 H_2^2}{B_2^2 B_1^2 H_2^2 H_1^2} \right\} \dot{Q} \tag{12}$$

When A_2 is greater then A_1 (the passage is divergent) and discharge $\dot{Q}$ is large enough thus Bernoulli resistance becomes negative [1, 2, 3]. It might happen that the net resistance also become negative thus the flow becomes unstable. This may lead to flow separation and the flow may latch on nearest stable pattern rendering zero Bernoulli resistance, as shown in the Fig.4.

To see the relative value of A_2 and A_1 we defined a term which may be called AxFlfact (axle flaring factor)

$$\text{AxFlfact} = \frac{\left(r_c + L\right)}{r_c} \times \frac{B_2}{B_1} \tag{13}$$

1. When $A_2 > A_1$, AxFlfact >1.0
2. When $A_2 = A_1$, AxFlfact =1.0
3. When $A_2 < A_1$, AxFlfact <1.0

D. Inertia of the fluid

Inertia of water in duct=I, Gap between two sides of duct at ξ distance from inner end of duct $H = H_1 + \alpha\xi$, Width of duct at ξ distance from inner end of duct $B = B_1 + \gamma\xi$

$$\text{Now I} = \int_0^L \frac{\rho}{A(\xi)} d\xi \tag{14}$$

$$\text{I} = \int_0^L \frac{\rho}{\left(H_1 + \alpha\xi\right)\left(B_1 + \gamma\xi\right)} d\xi$$

$$\text{I} = \rho \int_0^l \frac{d\xi}{\alpha\gamma(H_1/\alpha + \xi)(B_1/\gamma + \xi)}$$

$$\text{I} = \frac{\rho}{(B_1\alpha - H_1\gamma)} [\ln\{\frac{(H_1 + \xi\alpha)\gamma}{(B_1 + \gamma\xi)\alpha}\}]_0^l$$

$$\text{I} = \frac{\rho}{(B_1\alpha - H_1\gamma)} \ln(\frac{H_2 B_1}{H_1 B_2})$$

$$\text{I} = \frac{\rho L}{(B_1 H_2 - B_2 H_1)} \ln(\frac{H_2 B_1}{H_1 B_2}) \tag{15}$$

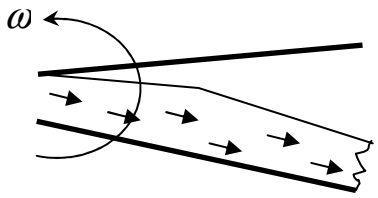

Fig.4: Assumed flow pattern.

E. Body forces

The body forces due to centrifugal forces works as the source of efforts on the fluid.

Body forces on the fluid referring Equation (1).

$$SE = \int_0^L B(\xi)\bar{e}_b(\xi).\bar{\eta}(\xi)d\xi \tag{16}$$

$$F_c = \rho r \varpi^2 \tag{17}$$

$$SE = \int_0^L \rho(r_c+\xi)\omega^2 d\xi \Rightarrow SE = \rho\omega^2\left[r_c L + \frac{L^2}{2}\right] \tag{18}$$

F. Reactive resistive torque

Torque = Rate of change of angular momentum

$$\tau = \rho\omega\dot{Q}(r_c + L)^2 + \rho\omega\dot{Q}r_c^2$$

$$\text{Reactive resistance} = \rho\dot{Q}(r_c+L)^2 + \rho\dot{Q}r_c^2 \tag{19}$$

The tangential motion of fluid flow through duct have very significant role. To study the effect of reactive resistance, we have introduced tangential flow factor (TanFlfact).We simulating the model for different values to see its significant on the motor performance. The factor determines tangential component of momentum transfer and thus reactive resistive torque on the motor.

Thus, Effective reactive resistance

$$=\text{TanFlfact}\times(\rho\dot{Q}(r_c+L)^2 + \rho\dot{Q}r_c^2) \tag{20}$$

G. Coriolis resistive torque

Coriolis resistive torque will develop due to Coriolis acceleration of fluid element [5].

$$\text{Coriolis acceleration} = 2\omega\times v \tag{21}$$

$$\text{Coriolis force on element } dF = 2\dot{r}\omega\rho 2r\sin\frac{\theta}{2}drB \tag{22}$$

$$\text{Torque on element } d\tau = 2\dot{r}\omega\rho 2r\sin\frac{\theta}{2}drBr$$

$$d\tau = 2\dot{r}\omega\rho 2r\sin\frac{\theta}{2}drBr \Rightarrow d\tau = 2\dot{Q}\omega\rho r dr \tag{23}$$

$$\tau = 2\dot{Q}\omega\rho\int_{r_c}^{(r_c+L)} r dr \Rightarrow \tau = \rho L^2\left(1+\frac{2r_c}{L}\right)\dot{Q}\omega$$

(24) Hence, Coriolis resistance $R = \rho L^2\left(1+\frac{2r_c}{L}\right)\dot{Q}$

The flow through duct is governed by viscous resistance, Bernoulli resistance, inertia and body forces on fluid. When the total resistance becomes negative flow will becomes unstable and in such situation, prediction of actual flow behaviors is very difficult. To consider all these effects on Coriolis resistive torque, we introduce Radial flow factor (RadFlfact) to find effective Coriolis resistance.

Thus effective Coriolis resistance

$$=\text{RadFlfact}\times\rho L^2\left(1+\frac{2r_c}{L}\right)\dot{Q} \tag{25}$$

H. Bond graph model of the rotating duct

Considering all above mentioned expressions for fluid flow governing equation and resistive torques, we created bond graph model of the duct in the form of capsule. Then we create the bond graph of rotating duct by adding the variable speed drive motor as a source of flow. It is based on flow characteristic of the duct and then combination of different modes of energy absorption in the duct like reactive resistance, Coriolis resistance.

Bond graph of the duct is represented as bellow Fig. 5.

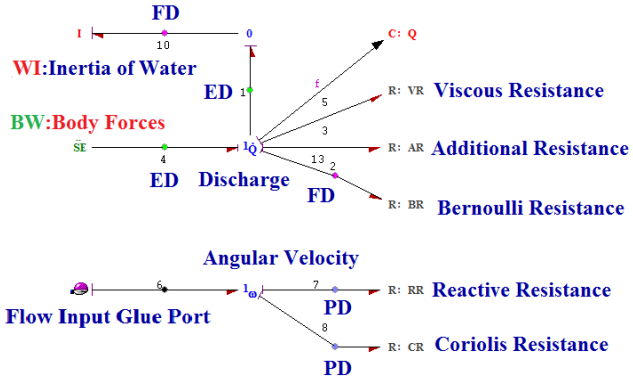

Fig. 5: Bond graph model (capsule) of the rotating duct.

In the above bond graph flow-input-glue-port at bond 6 depict angular velocity of the driving motor and effort detector (ED) on bond number 1, 4 detect effort in respective bond. The flow detector (FD) at bond 2, 10 detects the flow discharge rate of fluid. Likewise power detector (PD) at bond 7, 8 detect the power dissipated by the reactive resistance and Coriolis resistance respectively.

The bond graph model of the integrated system i.e. rotating duct with prime mover (motor) shown in Fig. 6. Power detector 1 is used to measure the power consumed by motor to rotate the duct. Driving motor is shown as source of flow.

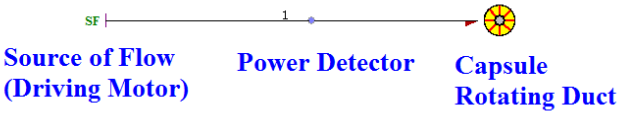

Fig. 6: Bond graph model of the rotating duct with motor.

IV. SIMULATION RESULTS AND DISCUSSIONS

The following input parameters are used as first set.

Table 2: Input parameters for simulation of bond graph model.

Density of water (kg/m^3)	1000.0
Dynamic viscosity of water (Pa-s)	0.001
Inner radius of duct (m)	0.1
Length of duct (m)	0.1
Width of duct at inner end (m)	0.05
Width of duct at outer end (m)	0.025
Tangential flow factor	0.6
Radial flow factor	0.9
Additional Resistance Factor	0.0
Angle between two vertical walls of duct (degree)	15.0
Angular speed of motor (RPM)	200.0

Various simulation results are obtained varying one input parameter at a time and assuming value of remains parameters as per table 1 to see the effect of that parameter on the power consumed by driving motor.

The Fig. 7(a) shows the motor power for first set of input parameters. Fig 7(b-h) shows the effect of variation of particular input parameter on motor power. It can be seen from Fig.7 (b) that as the duct length increases from 0.1 m to 0.30 m the power drawn by motor increases from 92.1 kW to 149.0 kW.

The effect of duct width is shown in Fig.7(c-d). Variation in duct width changes the area ratio at outlet to inlet of the duct. Till the B1 is equal to 0.05 m for B2 equal to 0.025 m the area ratio is less than one, Bernoulli resistance will be positive and it will reduce the fluid flow rate through the duct. So motor draw less power but as area ratio becomes more than one, Bernoulli resistance become negative in such case we assumed Bernoulli resistance equal to zero, thus flow rate will increases and motor will draw more power. The tangential flow factor controls the reactive resistive torque developed by the duct. The power drawn by the motor increases from 67.5 kW to 104.0 kW as the tangential flow factor increases from 0.2 to 0.8. The effect of radial flow factor is shown in Fig.7 (f). The power drawn from motor increases from 49.1 kW to 85.9 kW as radial flow factor increases from 0.2 to 0.8. It can be seen from Fig. 7(g) that as the angular speed of motor increases from 150 rpm to 225 rpm, power drawn from motor increases from 29.14 kW to 147.53 kW.

An effect of variation of the angle between vertical surfaces of duct is shown in Fig.7 (h). The power drawn by the motor increases 38.5 kW to 219.0 kW as the angle increases from 10.0 degree to 25.0 degree.

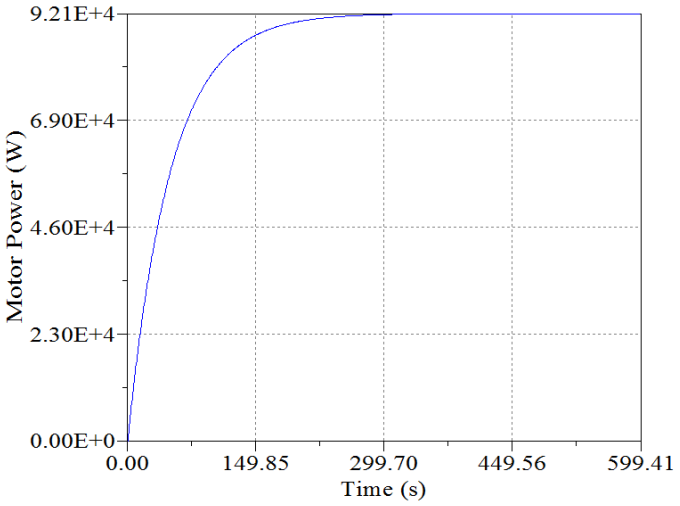

Fig. 7(a): Motor power for first set of input parameters.

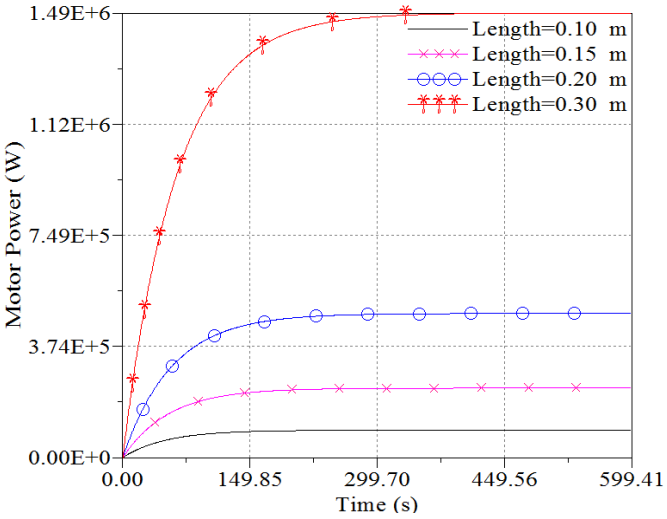

Fig. 7(b): Effect of the duct length

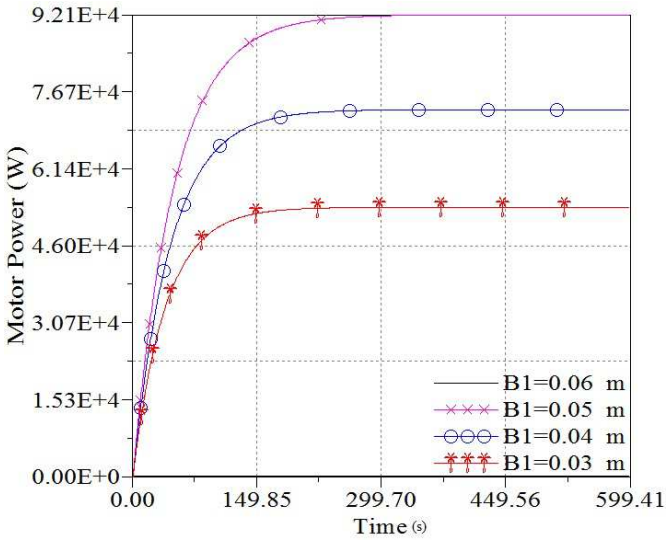

Fig. 7(c): Effect of the duct width at inlet.

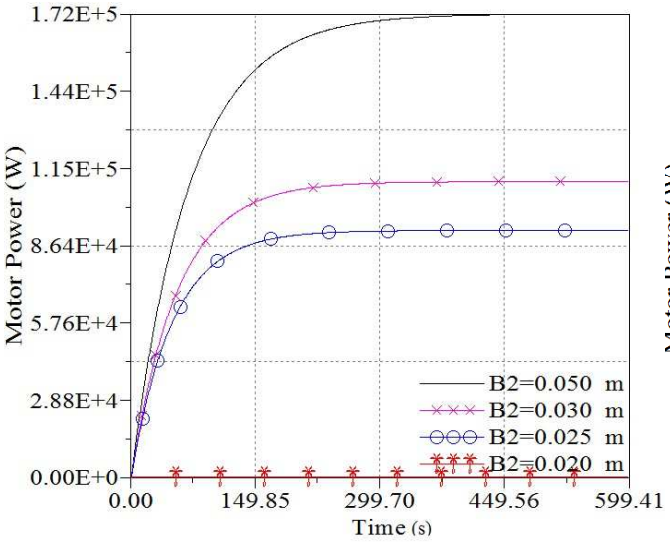

Fig. 7(d): Effect of the duct width at outlet.

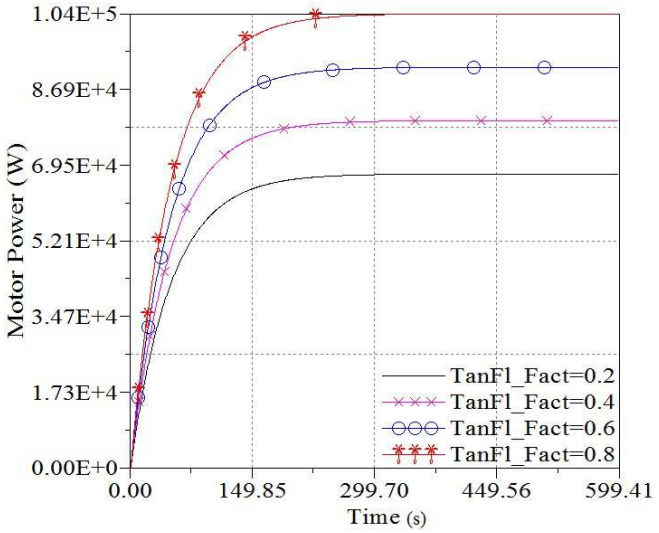

Fig. 7(e): Effect of tangential flow factor.

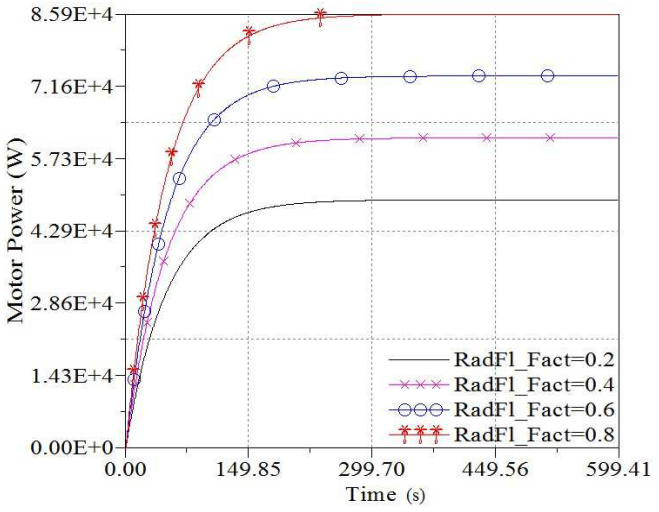

Fig. 7(f): Effect of radial flow factor.

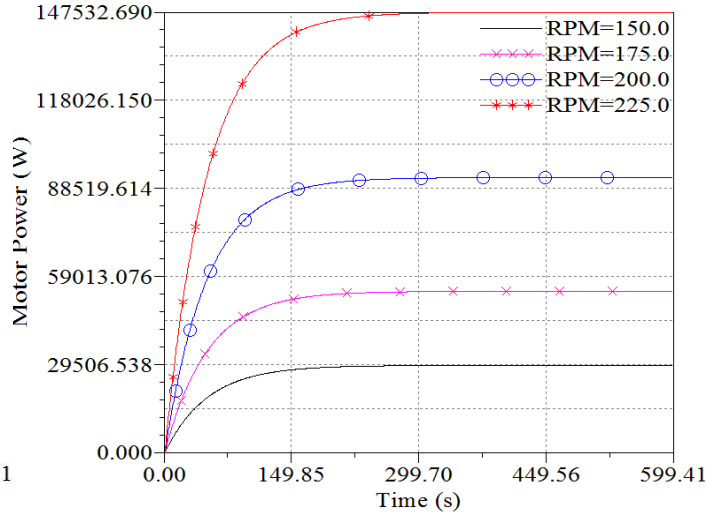

Fig. 7(g): Effect of angular velocity.

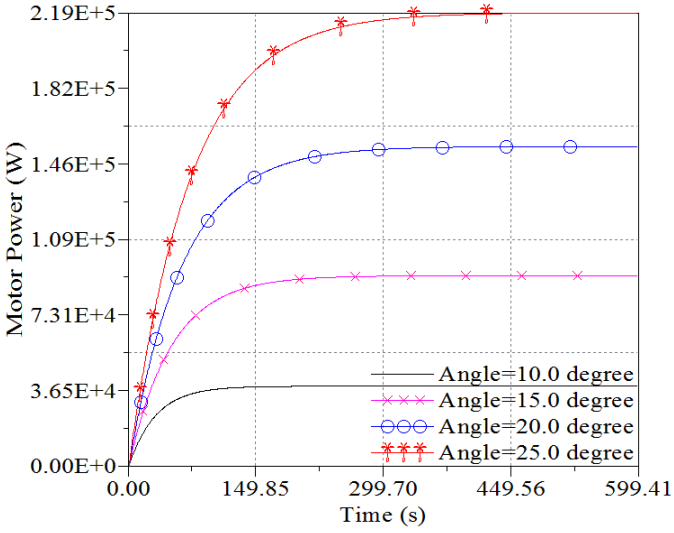

Fig. 7(h): Effect of angle between side surfaces.

Fig.7 (a-h): Simulation results

V. CONCLUSIONS

Modeling of the rotating duct through bond graphs has provided a deep insight into the dynamic behavior of the system. It helps us to study the effect of various design parameters of system on the performances of the motor, i.e. power require to drive the pump. However in this model the dynamic effects of rotating arrangement are neglected, these details can be taken as future scope of work.

ACKNOWLEDGMENTS

Authors gratefully acknowledge Prof A.K. Samantaray for his guidance and suggestions, and Mr. Naveen Thakur, Mr. Kanakendu Banerjee and Mr. Partha Mukherjee for their support, suggestions and writing assistance.

REFERENCES

[1] Amalendu Mukherjee, Ranjit Karmakar, and Arun Kumar Samantaray, "Bond Graph in Modeling, Simulation and fault Identification", I. K. International Publishing House Pvt. Ltd., 2005.

[2] Dean C. Karnopp, Donald L. Margolis, Ronald C. Rosenberg, "System Dynamics: A Unified Approach", John Wiley &Sons Inc., 1990.

[3] Frank M White, "Fluid Mechanics", Tata McGraw-Hill Publishing Company Limited, 2008.

[4] F. S. Jerome, J. T. Tseng, and L. T. Fan, "Viscosities of Aqueous Glycol Solutions", Journal of Chemical and Engineering Data, 1968.

[5] Pijush K. Kundu, Iram M. Cohen, "Fluid Mechanics", Elsevier, 2005.

[6] Michael David Bryant, "Physics review and bond graph:Fluidic Bond Graphs", University of Texas at Austin, 2002.

[7] Manual SYMBOLS Sonata (Release 3.0) 2009, HighTech Consultants, IIT- Kharagpur.